SI Appendix

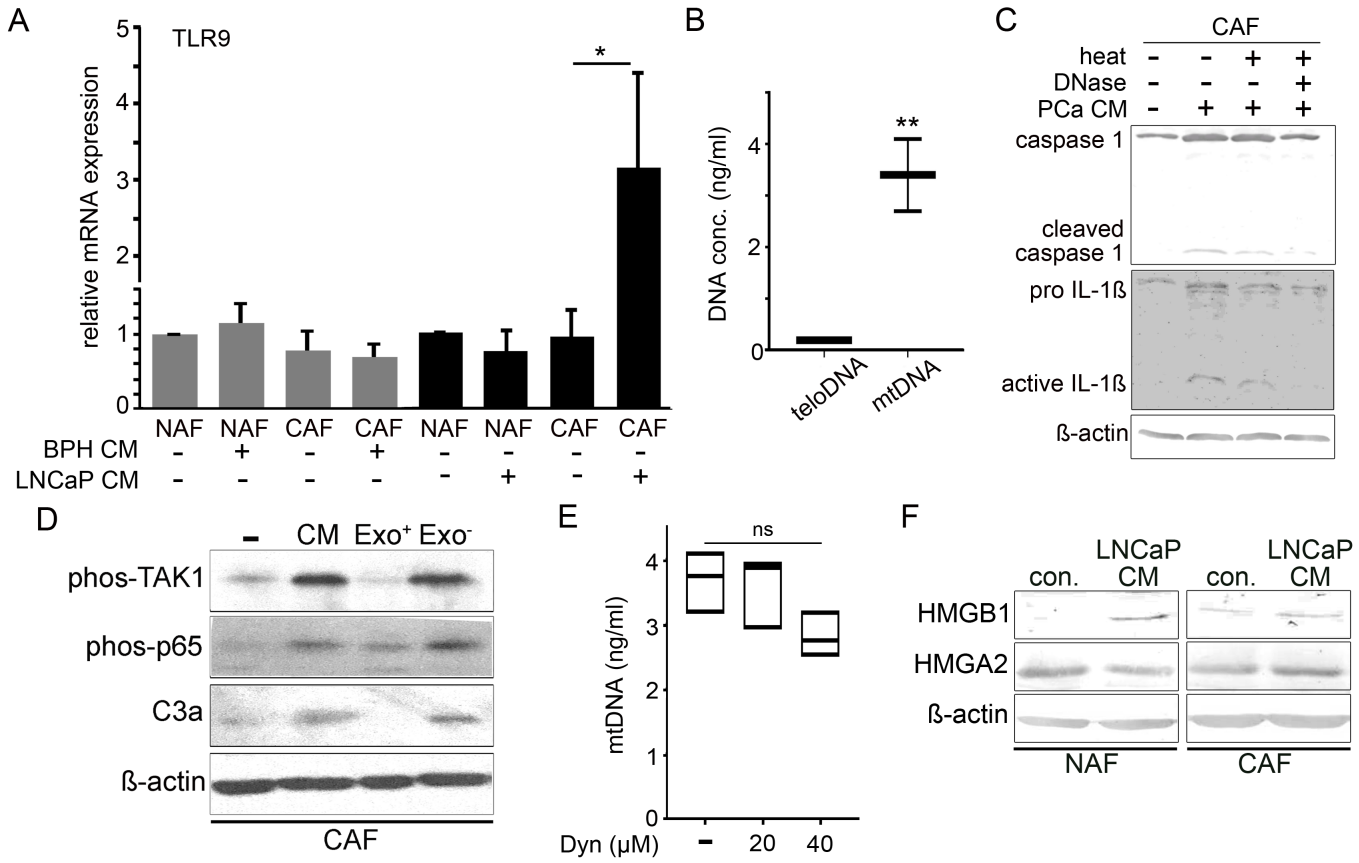

Figure S1. A Relative mRNA expression of TLR9 was measured in the presence and absence of BPH1 conditioned medium (CM) and LNCaP-CM in cultured NAF or CAF. **B** Measurement of telomere and mitochondrial DNA concentration from conditioned medium of cultured human prostate cancer cells. **C** Protein expression of caspase1 and IL-1β from cultured CAF treated with LNCaP-CM. Lower molecular weight cleaved-caspase1 and mature active-IL1β induced by LNCaP-CM was limited by DNase1 treatment and subsequent heat inactivation. ß-actin expression was used as a loading control. **D** Western blot for phosphorylated TAK1, phosphorylated p65, and C3a from CAF cells cultured with RPMI (-), LNCaP-CM (CM), exosome enriched RPMI (Exo^+), or exosome depleted LNCaP-CM (Exo^-). **E** Inhibition of dynamin-mediated exosome secretion with increasing doses of dynasore had no effect on the secretion of mtDNA by LNCaP cells. **F** Protein expression of HMGB1 and HMGA2 by NAF and CAF was subjected to western blotting following LNCaP-CM treatment. *P < 0.05, **P < 0.01, ***P < 0.001.

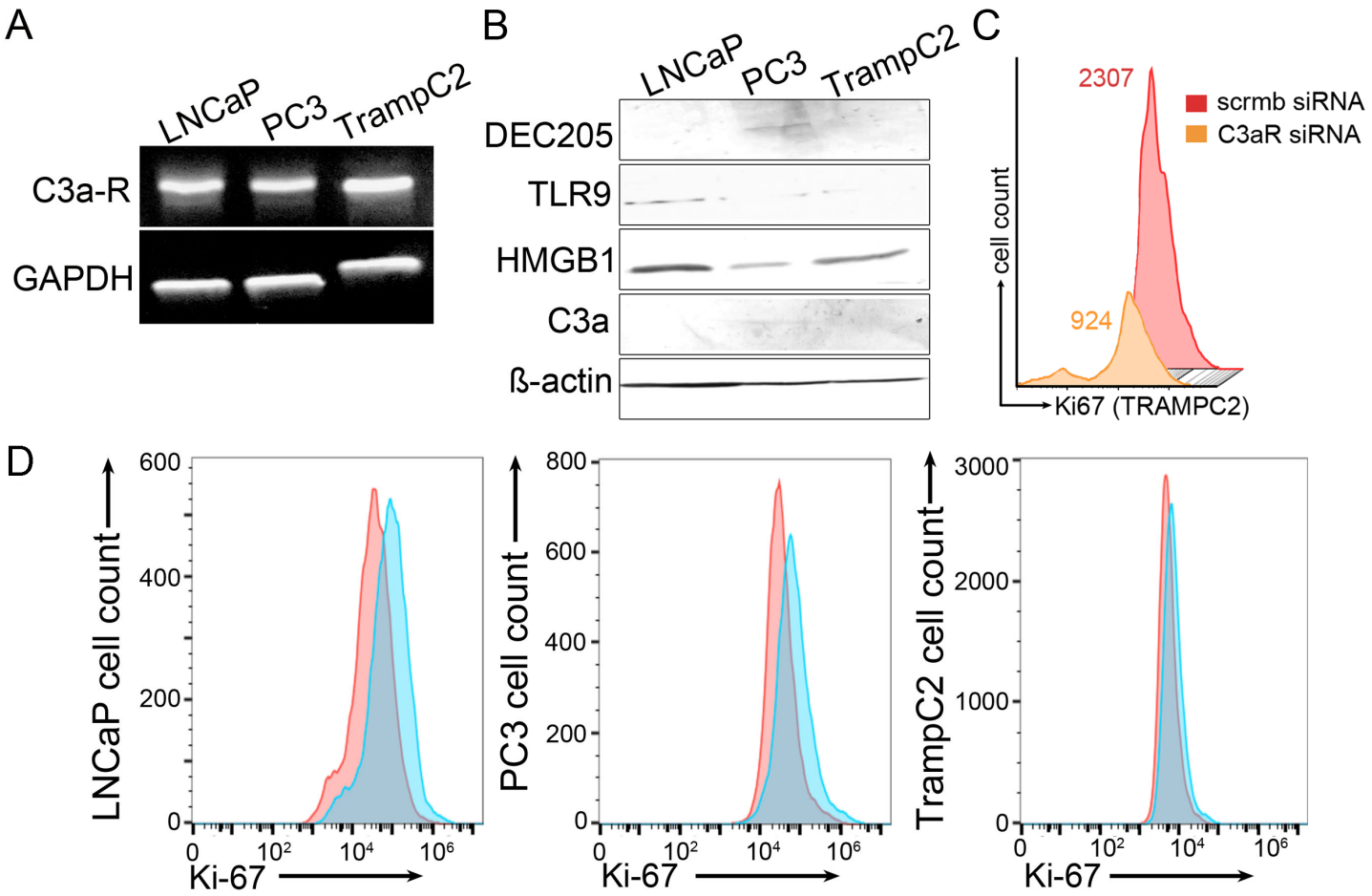

Figure S2. A C3a receptor (C3a-R) mRNA expression was similarly expressed by cultured LNCaP, PC3 and TrampC2 cells. **B** Western blot for the expression of DEC205, TLR9, HMGB1, and C3a was performed on the indicated PCa epithelial cell lines. **C** Scrambled or C3aR siRNA knockdown of TRAMPC2 cells were exposed to CAF cells in a trans-well co-culture for 48 h. Ki67 of TRAMPC2 was quantitated through FACS analysis. **D** Proliferation of LNCaP, PC3 and TrampC2 cells was quantitated by measuring Ki-67 through FACS analysis following treatment with C3aR agonist or scrambled peptides for 48 h, (n = 3).

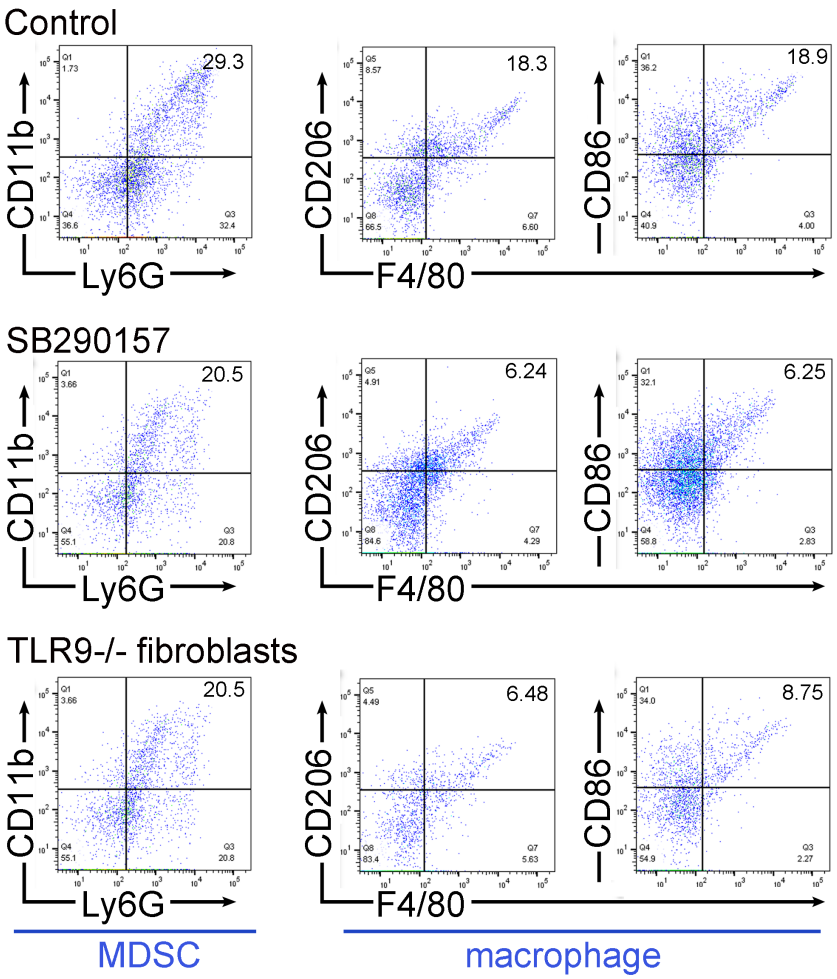

Figure S3. FACS analysis of the tumor draining lymph node from syngeneic mice with wild type prostatic fibroblasts or TLR9-knockout fibroblasts and TRAMPC2 epithelia (See Figure 3B). C3a antagonist (SB290157) and TLR9-knockout fibroblasts had similar reduction in the recruitment of myeloid derived cells (MDSC) and M2 macrophage activation, compared to control, saline treated mice harboring TRAMPC2/wild type prostatic fibroblasts tumors.

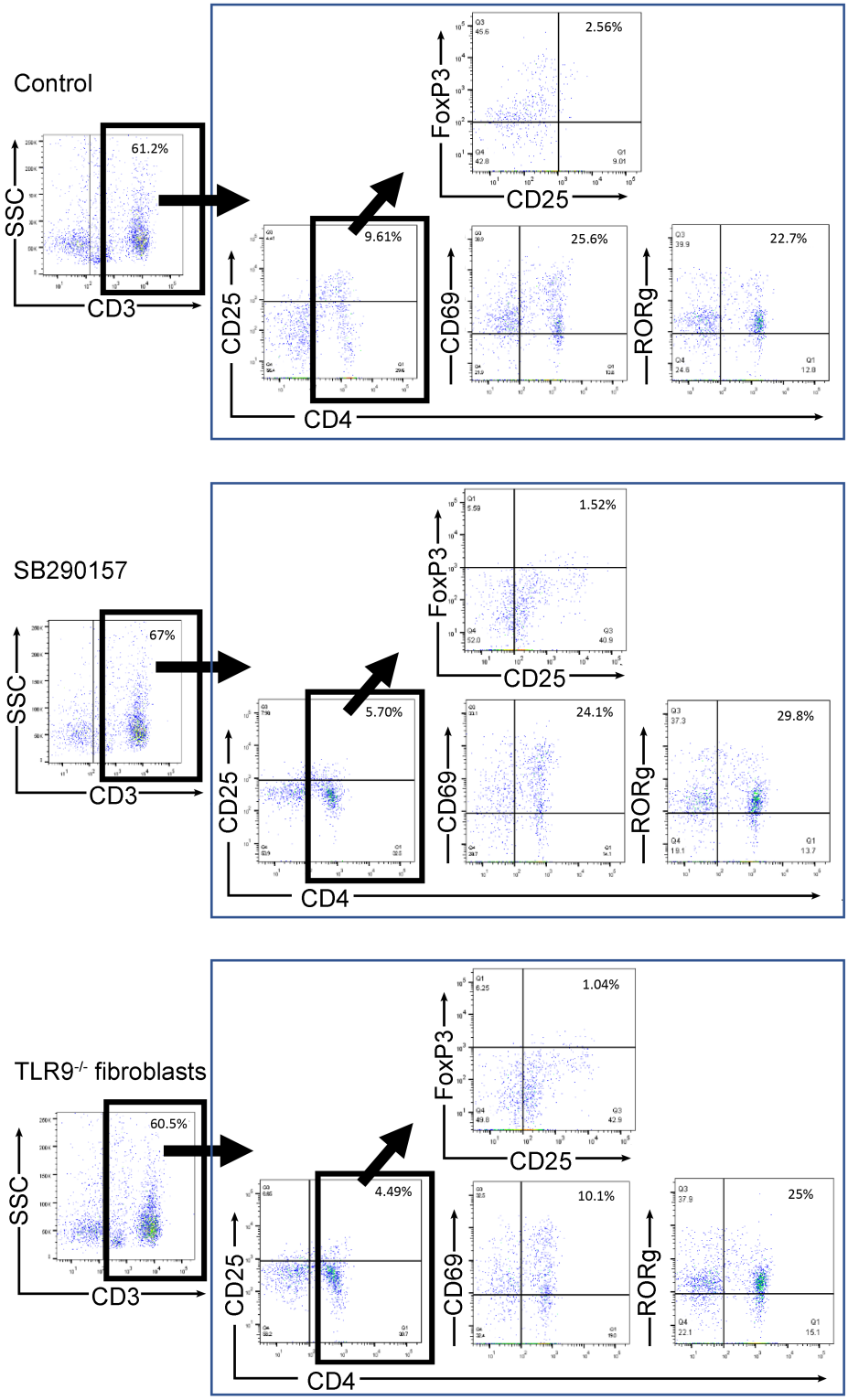

Figure S4. FACS analysis of the draining lymph node demonstrated C3a antagonist and TLR9-knockout fibroblasts had similar $CD3^+$ T cell infiltration, however the activation state of T helper cells, as determined by $CD4^+/CD69^+$ and $CD4^+/CD25^+$ expression differed significantly, compared to control. Th17 like cells ($CD4^+/ROR\gamma^+$) followed the opposite pattern with an increase in their presence in the C3 antagonist and the $TLR9^{-/-}$ fibroblasts models. In parallel we observed a decrease in T_{reg} (CD4+CD25+FoxP3+).

A

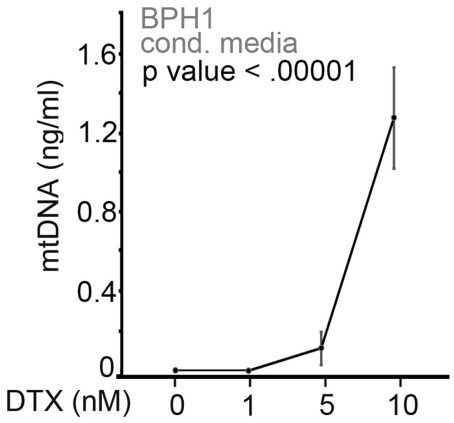

B

SB290157	Docetaxel	Interaction index	Lower bound Conf interval	Upper bound Conf interval
100	1	0.355	0.168	0.748
1000	10	0.129	0.054	0.309
10000	100	0.457	0.154	1.348
100	10	0.230	0.106	0.498
1000	100	0.760	0.287	2.011
1000	1	0.218	0.109	0.437
10000	10	0.096	0.038	0.242

C

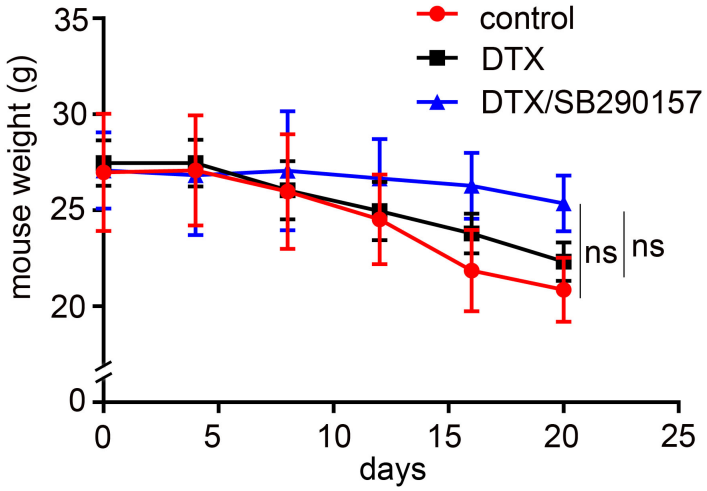

D

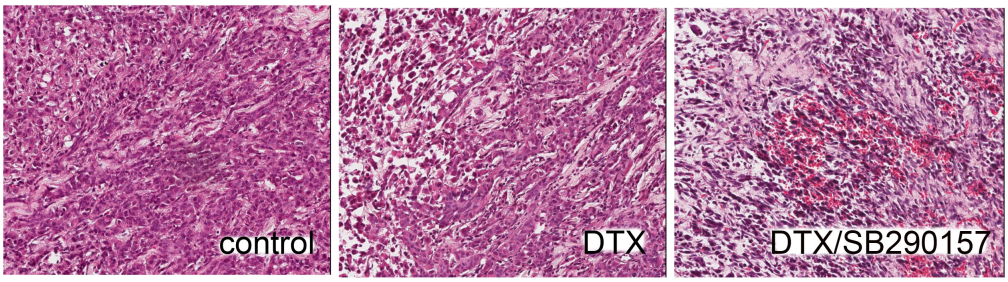

Figure S5. A MtDNA secreted by BPH1 cell line treated with docetaxel was elevated in a dose-dependent manner (n=3). Significance was determined by repeated measures ANOVA. **B** An interaction index and confidence intervals were calculated by Chou-Talalay method for determining a synergistic relationship between SB290157 and docetaxel treatment at the indicated treatment concentrations of PC3 cells by

the MTT viability assay. **C** Mice harboring subcutaneous xenografts of PC3/CAF tumors were weighed throughout the saline, docetaxel alone, or combination with SB290157 treatment course. Data represent the mean ± S.D. among groups by one-way ANOVA (ns - not significant). **D** H&E images of resulting tumors from each treatment group of subcutaneous xenografted mice.